Science of Sintering, **53** (2021) 223-235

https://doi.org/10.2298/SOS2102223M

UDK: 685.34.036; 541.128; 548.73; 691.73

A Possible Connection between Phosphate Tungsten Bronzes Properties and Briggs-Rauscher Oscillatory Reaction Response

Tijana V. Maksimović[1], Jelena P. Maksimović[2], Pavle I. Tančić[3], Nebojša I. Potkonjak[4], Zoran P. Nedić[2], Ljubinka G. Joksović[1], Maja C. Pagnacco[5*)]

[1]Department of Chemistry, Faculty of Science, University of Kragujevac, Radoja Domanovića 12, 34 000 Kragujevac, Serbia

[2]Faculty of Physical Chemistry, University of Belgrade, Studentski trg 12-16, 11001 Belgrade, Serbia

[3]Geological Survey of Serbia, Rovinjska 12, 11000 Belgrade, Serbia

[4]"Vinča" Institute of Nuclear Sciences - National Institute of the Republic of Serbia, University of Belgrade, Mike Petrovića Alasa 12-14, 11351 Belgrade, Serbia

[5]Institute of Chemistry, Technology and Metallurgy, University of Belgrade, Njegoševa 12, 11000 Belgrade, Serbia

Abstract:

The calcium phosphate tungsten bronze (Ca-PWB) has been synthesized and characterized (TGA, DSC, XRPD, FTIR, SEM). The influence of solid insoluble materials Ca-PWB, as well as lithium doped (Li-PWB) and cation free phosphate tungsten (PWB) bronzes on the oscillatory Briggs-Rauscher (BR) reaction dynamics, is compared. The results show that doping with Li and Ca reduces sensitivity of the BR reaction towards bronzes addition. These findings suggest the usage of the BR reaction as an innovative method for testing of different properties of bronze material. The behavior of PWB in the BR reaction is significantly changed with divalent cation (Ca^{2+}) doping. The reasons for the different bronzes behavior were found in their calculated unit cell volumes. Namely, the compressed Ca-PWB unit cell volume indicates the difficult availability of the active site for heterogeneous catalysis. Hence, the linear correlation (slope) of the BR oscillogram's length (τ_{osc}) vs. mass of bronze in BR reaction might be considered as a new parameter for the evaluation of the bronzes catalytic activity.

Keywords*: Briggs-Rauscher reaction; Phosphate tungsten bronzes; Keggin structures; Catalytic activity; Heterogeneous catalysis.*

1. Introduction

Heteropoly acids (HPAs) of Keggin's type having general formula $H_{(8-x)}XM_{12}O_{40}\times nH_2O$ (X^{x+} = P^{5+}, Si^{4+}, As^{5+}, Ge^{4+}, Ce^{4+}, Th^{4+} where x is oxidation number of X, M = Mo, W, V, Nb and n = 6-31) are principally interesting because of their high protonic conductivity at room temperature [1-3]. Additionally, thermal treatment of HPAs with Keggin's structures is the easiest, simplest and quickest method for obtaining phosphate tungsten bronzes (X = P, and M = W) [4]. Replacement of WO_6 octahedra in a structure of

*) **Corresponding author:** maja.pagnacco@nanosys.ihtm.bg.ac.rs

ReO_3-type showed the presence of two families of such intercalated compounds: monophosphate tungsten bronzes with pentagonal tunnels (MPTBp) or with hexagonal tunnels (MPTBh) where one WO_6 octahedron is substituted with PO_4 tetrahedron leading to monophosphate tungsten bronzes and diphosphate tungsten bronzes with hexagonal tunnels (DPTBh), where two adjacent WO_6 octahedron sharing corners are substituted with P_2O_7 diphosphate group [5]. This work deals with monophosphate tungsten bronzes (PWB), contributing to interesting correlations between their catalytic properties and crystal structure. Additionally, the three-dimensional network structure of PWB shows a metallic character [6-9]. The ability of bronze cavities to accommodate guest ions [5, 10-12] is employed in this work for synthesis and characterization of novel Ca-doped phosphate tungsten bronze (Ca-PWB) obtained in the process of high-temperature transformation of 12-tungstophosphoric acid calcium salt (Ca-PWA).

The potential application of phosphate tungsten bronzes is in their installation in batteries as electrode material [12], as well as catalysts for the oxidation process in fuel cells [13]. Besides bronzes usage as a pigments in traditional ceramics [14, 15], recent investigation by Moore and coworkers, of WO_3-TiO_2-P_2O_5 glass-ceramics system recognized phosphate-tungsten bronze as main responsible for this system exhibiting high electrical conductivity [16]. Namely, it was shown that the conducting phases in tungsten-titanium-phosphate glass-ceramics system have been identified as phosphate tungsten bronzes, rather than tungsten suboxides. In general, PWB metallic properties and the high oxidation state of tungsten, make this material as a promising catalyst in the Briggs-Rauscher (abbreviated as BR) oscillatory reaction [17, 18]. The BR reaction is one of the most interesting oscillatory reaction where the oxidation of malonic acid [$CH_2(COOH)_2$], in the presence of hydrogen peroxide (H_2O_2) and potassium iodate (KIO_3), is catalyzed by manganese ions (Mn^{2+}) in acidic medium [19]:

$$IO_3^- + 2H_2O_2 + CH_2(COOH)_2 + H^+ \rightarrow CHI(COOH)_2 + 2O_2 + 3H_2O \quad (1)$$

The oscillatory chemical reactions are complex dynamic systems, in which the concentrations of reactants and products cascadingly grow and fall by the change of intermediate concentration, reflecting the periodical changes in rate of their evanescence, i.e. the rate of their formation [20, 21]. There are at least two methods for complex oscillatory system study: *i*) the investigation of their chemical subsystems [22-26] and *ii*) the investigation of oscillatory system behavior under different perturbants [21, 27-30]. The BR reaction is sensitive to many organic molecules (for example, antioxidants). Their presence in the BR system influences the dynamic state by disordering the oscillatory evolution of the system [27, 28]. Thus, this reaction is often used for quantitative intents or for measuring antioxidant/antiradical activity [27]. Our recent investigation shows that the BR reaction could be used for distinction of different types of bronzes (e.g. phosphate tungsten and phosphate molybdenum) based on their different catalytic activity [17].

This work further investigates the potential of the BR system to distinguish doped and undoped (cation free) phosphate tungsten bronzes and correlates their catalytic activity in the BR reaction with their structural properties.

2. Materials and Experimental Procedures

2.1 Synthesis of Calcium doped phosphate tungsten bronze (Ca-PWB)

Heteropoly acid hydrate $H_3PW_{12}O_{40}\times29H_2O$ (PWA) was obtained by dissolving $Na_2WO_4\times2H_2O$ in a H_3PO_4-HCl mixture and by extracting the precipitate with ether at room temperature [31]. The dehydration process of $H_3PW_{12}O_{40}\times29H_2O$ (PWA) to $H_3PW_{12}O_{40}\times6H_2O$ (6-PWA) is done by heating of PWA in a kiln at 80 °C [10]. Aqueous

solution of $H_3PW_{12}O_{40}\times 6H_2O$ is commingled with aqueous solution of $CaCl_2\times 2H_2O$, slightly heated in order to start the process of crystallization and left during the night to finish the crystallization. The obtained acidic salt $CaHPW_{12}O_{40}\times 6H_2O$ (Ca-PWA) is then heated in a furnace (the velocity of heating is 10 °C min^{-1}), in temperature range from room temperature to 590 ^oC, whereby the light-green crystals of calcium doped phosphate tungsten bronze are formed.

2.2 Thermal analyses (TA)

Thermal examinations were performed using TA Instruments STD 2960 Simultaneous DSC-TGA using a higher scanning rate (10°C min^{-1}), from room temperature to 800 ^oC in a stream of nitrogen.

2.3 X-ray powder diffraction (XRPD)

X-ray powder diffraction (XRPD) patterns were obtained using a Rigaku Ultima 4 automated diffractometer with a Cu tube operating at 40 kV and 40 mA. The instrument was provided with a curved graphite monochromatic diffraction beam, and Xe-filled proportional counter. The diffraction data were collected in the 2θ Bragg angle ranges from 10 to 90^o, counting for 2 deg min^{-1} at every 0.05^o steps. The divergence and receiving slits were fixed at 0.5° and 0.15 mm, respectively. The XRPD measurements were performed ex situ at room temperature (23 ^oC) in a stationary sample holder. Diffractometer alignment was checked by means of a standard Si powder material. Calculations of the unit cell dimensions were accomplished by the LSUCRI program [32].

2.4 Fourier Transform Infrared Spectroscopy (FTIR)

FTIR spectra were recorded on a Thermo Scientific Nicolet 6700 using KBr pellet technique with 64 scan and 2 cm^{-1} resolution.

2.5 Scanning Electron Microscopy (SEM)

Investigations of the crystal morphology were carried out with a scanning electron microscopy (SEM JSM 840A, Jeol). The Ca-PWA and Ca-PWB samples were gold-coated for SEM study.

2.6 Briggs-Rauscher reaction – Experimental Setup

All experiments are carried out in a stationary, isothermal and well-mixing reactor (σ = 900 rpm). The reaction volume was 25.0 ± 0.1 ml. The initial concentrations of the reactants in the system were: $[CH_2(COOH)_2]_0$ = 0.0789 mol dm^{-3}, $[MnSO_4]_0$ = 0.00752 mol dm^{-3}, $[HClO_4]_0$ = 0.03 mol dm^{-3}, $[KIO_3]_0$ = 0.0752 mol dm^{-3} and $[H_2O_2]_0$ = 1.269 mol dm^{-3}. The experimental equipment and procedure were the same as described in reference [17], where the method for solid insoluble sample is established for the first time. After reaching of the desired temperature (37.0 ^oC) and stabilization of the potential of Pt working electrode, appropriated masses of calcium doped phosphate tungsten bronze (0.0138 g ± 0.0001 g; 0.0179 g ± 0.0001 g; 0.0268 g ± 0.0001 g; 0.0308 g ± 0.0001 g; 0.0558 g ± 0.0001 g; 0.0737 g ± 0.0001 g; 0.0956 g ± 0.0001 g; 0.1110 ± 0.0001 g), have been appended into the reaction system. When the metal catalyst Mn^{2+} in the form of $MnSO_4$ was tested, homogeneous conditions, the experiments were performed in the same way as the basic BR system without

the addition of analytes, but with different concentrations of $MnSO_4$ (0.00752 mol dm^{-3}, 0.04866 mol dm^{-3}, 0.0784 mol dm^{-3} and 0.0898 mol dm^{-3}).

3. Results and Discussion

3.1 Characterization of 12-tungstophosporic acid calcium salt (Ca-PWA) and calcium doped phosphate tungsten bronze (Ca-PWB)

The results of thermal analysis of $CaHPW_{12}O_{40}\times 6H_2O$ from room temperature to 827 ^oC are presented in Fig. 1. The DSC curve shows two endothermic peaks at 50 ^oC and 170 ^oC and one exothermic at about 590 ^oC. When the sample loses molecules of water, anhydrous phase of $CaHPW_{12}O_{40}$ is formed. The exothermal process corresponds to solid-solid transformations of Keggin's anions and bronze formation.

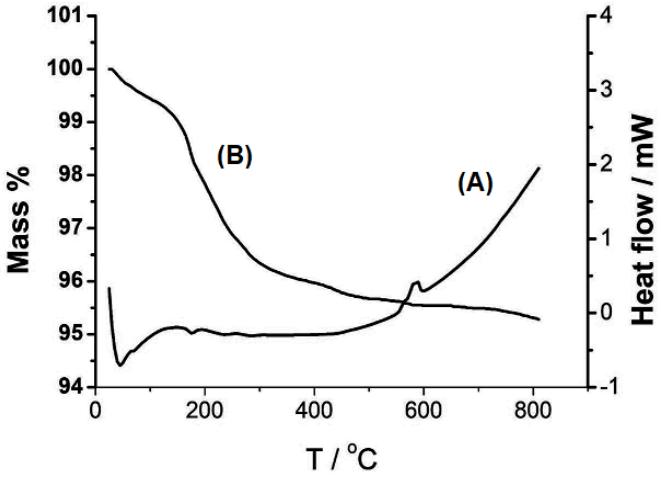

Fig. 1. (A) DSC and (B) TGA curves of $CaHPW_{12}O_{40}\times 6H_2O$.

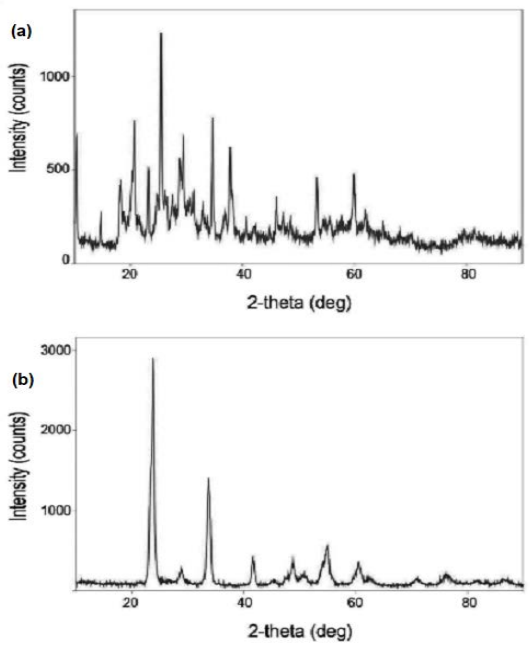

Fig. 2. XRPD patterns of: (a) Ca-PWA and (b) Ca-PWB.

The XRPD patterns of Ca doped phosphate tungsten acid (abbreviated as Ca-PWA) and Ca-PWB are shown in Fig. 2 and Table I. The obtained data denote that these two studied samples are appealingly very different. The main reason is their structural differences and the phase temperature transition. Particularly, the data for Ca-PWA are quite similar to those obtained for the cubic stable phase determined as 6-PWA which was calcined at 170 ^{o}C [10], but with somewhat different intensities for the strongest peaks and background, as well.

Tab. I Inter-planar spacing (*d*, in Å) and intensity (*I*, in %) of Ca-PWA and Ca-PWB.

Ca-PWA[(b)]		6-PWA[(a)]			Ca-PWB[(b)]		PWB[(a)]			Li-PWB[(b)]			
d	I	d	I	h k l	d	I	d	I	h k l	d	I	$d_{cont.}$	$I_{cont.}$
8.55	37	8.58	66	1 1 0	3.81	33	3.84	41	0 0 2	6.55	3	1.80	10
6.05	11	6.07	16	2 0 0	3.72	100	3.75	100	0 2 0	6.12	2	1.71	9
4.93	88	4.96	15	2 1 1	3.09	13	3.11	6	-1 1 2	3.83	100	1.69	7
4.28	100	4.30	36	2 2 0	2.66	64	2.68	40	-2 0 2	3.75	81	1.67	9
3.84	19	3.84	24	3 1 0			2.64	26	2 0 2	3.64	85	1.64	16
3.60	29				2.17	12	2.17	14	-2 2 2	3.49	3	1.53	5
3.50	69	3.51	100	2 2 2	1.99	3	2.01	2	2 1 3	3.34	15	1.49	8
3.10	37				1.86	18	1.87	11	-1 0 4	3.08	15	1.39	2
3.04	21	3.04	29	4 0 0	1.79	12	1.81	4	-1 1 4	2.68	29	1.31	3
2.87	25	2.87	13	3 3 0	1.67	40	1.67	15	-2 1 4	2.61	42	1.24	5
2.59	40	2.59	51	3 3 2	1.53	18	1.53	9	2 4 2	2.52	5	1.18	3
2.44	19				1.48	7	1.49	3	-1 4 3	2.17	9	1.16	3
2.38	54	2.38	23	5 1 0	1.32	6				2.15	10	1.13	3
2.22	5	2.22	5	5 2 1	1.25	14				2.04	2		
1.97	59	1.97	13	6 1 1						1.98	5		
1.72	25	1.72	20	7 1 0						1.92	7		
1.54	35	1.54	18	6 5 1						1.88	8		
1.50	13	1.50	8	8 1 1						1.82	18		

(a) Ref [10], (b) this paper

Likewise, the data for Ca-PWB are analogical to those obtained for PWB crystallized as monoclinic at temperature conditions of 750 ^{o}C [10]. It can be also emphasized here that peaks with the highest intensities for Ca-PWB (i.e. at about 23-24^{o} and 33-34^{o} 2θ, Fig. 2b) have no such visible doublets as PWB, but only shoulders and extra-broadening. Contrariwise, this calcium derivative significantly differs from its Li analog synthesized at the same temperature of 650 ^{o}C (Table I), which is most probably orthorhombic or triclinic [12]. It could be also significant for some future studies that these Ca-PWB, Li-PWB and PWB compounds were formed at considerable lower temperatures than other different phosphate tungsten bronzes varieties (with m = 2, 6 and 7) within the WO_3-TiO_2-P_2O_5 system, which are formed above 850 or 950 ^{o}C [16].

At Table I, inter-planar spacing and intensities for Ca-PWA and Ca-PWB were compared to 6-PWA ($H_3PW_{12}O_{40}\times 6H_2O$) and PWB with their adequate Miller's hkl indices presented [10]. Data for Li-PWB [12] are also added for comparison, but without adequate Miller's hkl indices presented, having in mind that its structure is not yet resolved.

In order to additionally compare cation free and doped phosphate tungsten bronzes, unit cell dimensions of PWB, Li-PWB and Ca-PWB were calculated on the basis of the hypothetically assumed triclinic symmetry (PW_8O_{26} phase, [10], Table II). From the presented results, it can be seen that compression of the unit-cell dimensions of PWB occurred, when Li and Ca were inserted into the structures of Li-PWB and Ca-PWB. Decreasing of the unit cell volume of Ca-PWB is even more expressive than for the Li-PWB, in spite that Ca^{2+} ion is considerable larger than Li^{+}.

Tab. II Calculated unit cell dimensions of PWB, Li-PWB and Ca-PWB.

	PWB[(a)]	Li-PWB[(b)]	Ca-PWB[(b)]
a_0 (Å)	7.310(1)	7.300(3)	7.332(5)
b_0 (Å)	7.524(1)	7.513(3)	7.469(9)
c_0 (Å)	7.686(1)	7.696(2)	7.630(3)
α_0 (^{o})	88.90(1)	87.83(6)	88.06(7)
β_0 (^{o})	90.98(1)	91.51(3)	90.57(6)
γ_0 (^{o})	90.94(1)	90.27(3)	90.5(1)
V_0 (Å^3)	422.5(1)	421.7(2)	417.6(5)

[(a)]Ref [10] [(b)]this paper

The FTIR spectra of polycrystalline Ca-PWA at room temperature are shown in Fig. 3. In the Ca-PWA spectrum we can notice characteristic bands of PO_4 tetrahedral, WO_6 octahedral and molecule H_2O. The band at 1650 cm^{-1} corresponds to ν_2 (H_2O) bending vibration of water. IR characteristic bands of the Keggin's anion structure were: the band at 1080 cm^{-1} belongs to ν_3 (PO_4) vibration, the band at 980 cm^{-1} corresponds to vibration of ν_1 (PO_4) tetrahedron, the band at 890 cm^{-1} corresponds to ν (W = O) vibration, the band at 800 cm^{-1} confirms the vibration ν (O-W-O), the band at 595 cm^{-1} can be attributed to the vibration ν_4 (PO_4) of the tetrahedron and the band at 510 cm^{-1} corresponds to the ν_2 (PO_4) vibration. In the process of calcination, the definite changes are evident and the destruction of Keggin's ions bronze is formed (Ca-PWB). According to the performed experimental investigations, after phase transformation at 590 ^{o}C, Ca-PWA switches to Ca-PWB. The obvious changes are in agreement with the X-ray diffractograms (Fig. 2). The definitive changes are apparent after destroying Keggin's anion (FTIR spectra in Fig. 3b). The band assignment with respect to the PO_4 tetrahedron and the WO_6 octahedron was also performed.

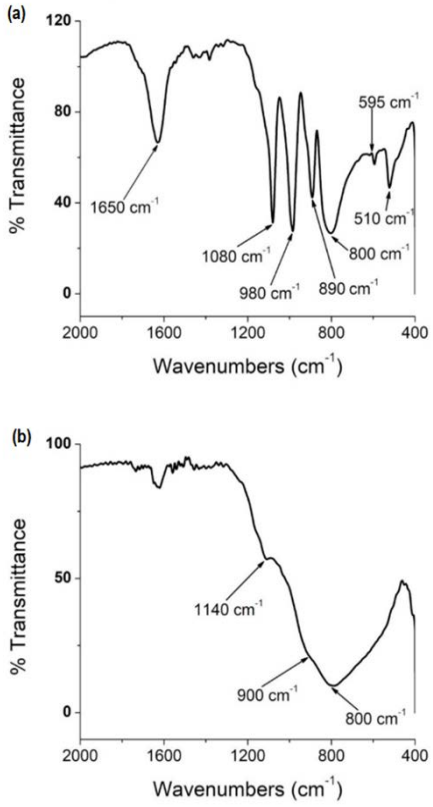

Fig. 3. FTIR spectra of: (a) Ca-PWA and (b) Ca-PWB.

The medium intensity band ν_3 (1140 cm^{-1}) is characteristic for the PO_4 group while the band at 900 cm^{-1} and very strong band at 800 cm^{-1} are characteristic for WO_6 octahedron. This indicates that the new structure corresponds to the composite WO_3 oxide. Phosphorus is in the form of PO_4 at a very small percentage relative to WO_3, with the PO_4 group contributing to the stability of WO_3. However, there is also the possibility of building a mixed network consisting of WO_6 octahedra and PO_4 tetrahedra.

As it is shown in Fig. 4, the morphology and microstructure of Ca-PWA (Fig. 4. a-b) and Ca-PWB (Fig. 4. c-d) products were observed by SEM images, respectively. The crack process in Ca-PWA crystals had followed the appearance of smaller crystals with the average size of several micrometers (~ 2 μm). Concerning Ca-PWB sample, SEM image have shown increased micrometer size (~ 20 μm) due to agglomeration of crystals [33-36].

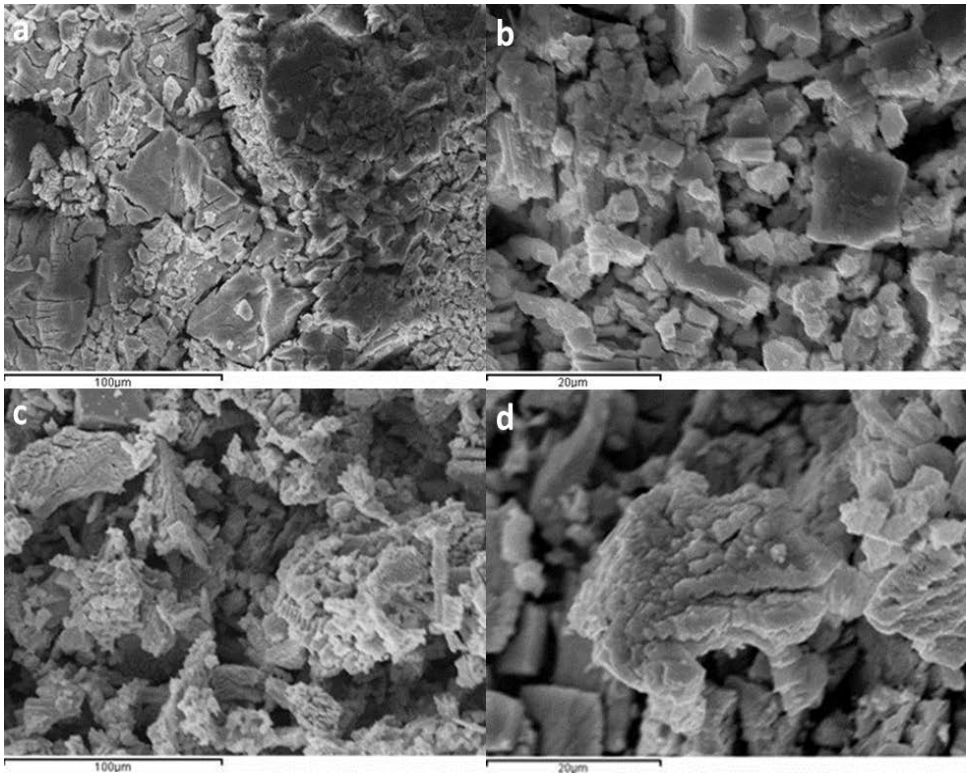

Fig. 4. SEM micrograph of: (a-b) Ca-PWA, (c-d) Ca-PWB.

3.2 Influence of Ca-PWB on BR reaction dynamics

The Fig. 5 represents oscillogram of the BR reaction by platinum electrode without the addition of Ca-PWB or basic BR oscillogram (a), and oscillograms in the presence of different masses of Ca-PWB: (b) 0.0138 g; (c) 0.0179 g; (d) 0.0268 g; (e) 0.0308 g; (f) 0.0558; (g) 0.0737 g; (h) 0.0956 g; and (i) 0.1110 g. It is shown that an increase of the mass of Ca-PWB does not lead to the significant change of the basic BR oscillogram.

It can be seen that the addition of different masses of Ca-PWB has as a negligible effect on the BR oscillogram's length (τ_{osc}). However, the added Ca-PWB mass above 0.0737 g started to influence the BR oscillatory dynamics changing the form of basic BR oscillogram and indicating the existence of a critical Ca-PWB mass which will still affect the BR kinetics, (*h)* and (*i)* in Fig. 5. This resulted in a negative slope obtained for τ_{osc} *vs.* mass function ($\tau_{osc} = -136 \times m_{CaPWB} + 98$, Fig. 6). The general conclusion is that the addition of different masses of Ca-PWB leads to scattering of the oscillatory period length around the basic BR

oscillogram, with a very small negative slope which neither can be used for the calibration curve nor for further quantitative determination of the unknown mass of Ca-PWB.

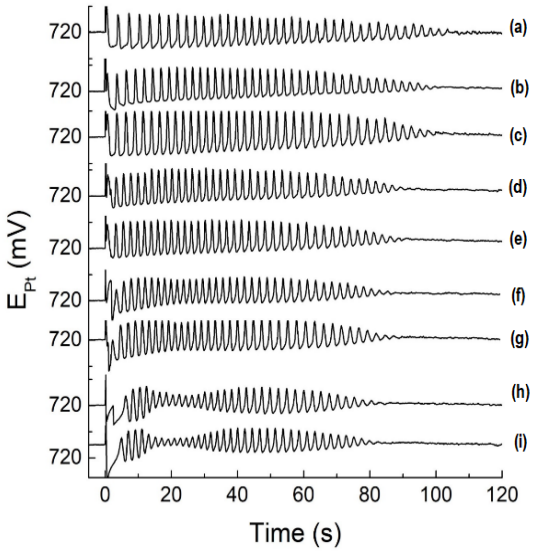

Fig. 5. BR oscillograms without Ca-PWB (a) and in the presence of different masses of Ca-PWB (b-i).

3.3 Comparison of undoped PWB, Li-PWB and Ca-PWB effects on oscillatory BR reaction dynamics

The effects of three tungsten bronzes, one undoped, Li^+ and Ca^{2+} doped, on BR oscillatory time duration as a function of added bronzes mass, are presented in Fig. 6. In all cases the linear correlation has been obtained:

PWB: $\tau_{osc} = -1289 \times m_{PWB} + 95$;
Li − PWB: $\tau_{osc} = -1083 \times m_{Li-PWB} + 97$;
Ca − PWB: $\tau_{osc} = -136 \times m_{Ca-PWB} + 98$.

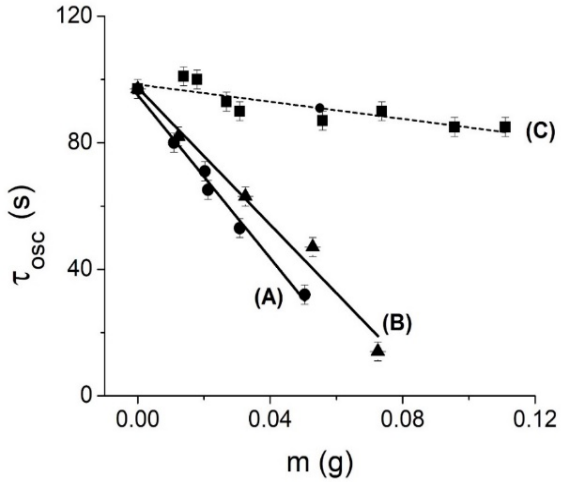

Fig. 6. Briggs-Rauscher oscillatory time, τ_{osc} *vs.* added bronzes mass for (A) PWB, (B) Li-PWB and (C) Ca-PWB.

The first two linear correlations can be used as calibration curve determining the unknown mass of bronzes and have been previously published [17, 18]. Namely, comparing cation-free, PWB, Li^+, and Ca^{2+} doped PWB behavior (all in heterogeneous conditions) in BR chemical system, it can be concluded that PWB shows the highest slope of τ_{osc} *versus* mass (Fig. 6). The obtained results evidently show that doping with Li and Ca reduces sensitivity (decrease the slope of τ_{osc} *vs* mass curve) of BR reaction towards bronzes addition. Furthermore, the doping with a divalent cation Ca^{2+} significantly changes the cation-free behavior of PWB in the BR oscillatory reaction. Consequently, what could be the potential reason for such behavior?

3.4 Doped and undoped phosphate tungsten bronzes as a heterogeneous catalysts in oxidation process involving hydrogen peroxide

The Keggin's type compounds and their derivate bronze could act as a catalyst, particularly for the oxidation process involving hydrogen-peroxide [13, 37]. Our recent investigation with PWB and phosphate molybdenum bronze (PMoB), indicates PWB bronze catalytic activity towards hydrogen peroxide even under heterogeneous conditions [17]. This fact is supported by the effects obtained on cyclic voltammograms of hydrogen peroxide with and without PWB. Furthermore, the addition of metal catalyst Mn^{2+} in the form of $MnSO_4$, homogeneous conditions, exhibits the same trend and negative slope as tungsten phosphate bronzes addition in BR (Fig. 7).

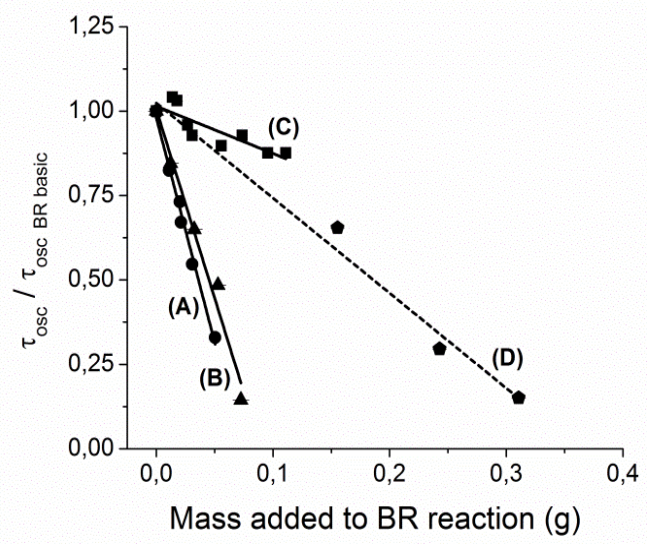

Fig. 7. The catalytic effects of (A) PWB, (B) Li-PWB, (C) Ca-PWB (catalytic action applied under heterogeneous conditions), (D) $MnSO_4$ (catalytic action applied under homogeneous condition) on BR oscillatory time duration.

It should be emphasized, there is applied the same methodology as for bronzes. The BR basic oscillogram still contained Mn^{2+} in form of $MnSO_4$ as described in the experimental section and the additional amount of $MnSO_4$ are presented in Fig. 7. The relative value of BR oscillogram, relating to the duration of BR oscillograms divided with basic BR oscillogram ($\tau_{osc}/\tau_{osc\ BR\ basic}$) in a particular set of measurements, is shown at ordinate with corresponding equations:

PWB: $\tau_{osc}/\tau_{osc\ BR\ basic} = -13.3 \times m_{PWB} + 0.98$

$\mathbf{Li-PWB}$: $^{\tau_{osc}}/_{\tau_{osc\ BR\ basic}} = -11.2 \times m_{Li-PWB} + 1.00$
$\mathbf{MnSO_4}$: $^{\tau_{osc}}/_{\tau_{osc\ BR\ basic}} = -2.8 \times m_{MnSO_4} + 1.02$
$\mathbf{Ca-PWB}$: $^{\tau_{osc}}/_{\tau_{osc\ BR\ basic}} = -1.4 \times m_{Ca-PWB} + 1.01$

The mass of added $MnSO_4$ determines the criterion for slope $^{\tau_{osc}}/_{\tau_{osc\ BR\ basic}} = -2.8 \times m_{MnSO_4} + 1.02$ that will be used for the efficiency of the catalyst. If the slope with a catalyst in BR reaction is larger than the slope obtained for $MnSO_4$, then the investigated catalyst has promising properties for the further investigation of the oxidation process involving hydrogen peroxide. Otherwise, the catalyst should not be further considered. As it can be seen, the PWB and Li-PWB showed better catalytic activity than $MnSO_4$ itself ((D) line in Fig. 7). Therefore, the catalyst with a slope higher than arbitrary slope recalculated for $MnSO_4$ catalyst is strongly recommended for the oxidation process involving hydrogen-peroxide. Obviously, the different catalytic activity by using cation-free and Li and Ca doped phosphate tungsten bronzes is responsible for obtained effects on BR oscillatory dynamics. Due to the all bronzes have the same basis (phosphate tungsten) the reasons for the different catalytic activity should be found in their structural properties.

3.5 Connection between bronzes' properties, catalytic action and BR reaction response

Bronzes with similar structures, such as Ca-PWB and PWB, have different effects on BR reaction (Table 1). On the other hand, bronzes with different structures, such as PWB and Li-PWB, have similar BR behavior. The most probable reason for such phenomenon could be found from the calculated unit cell volumes (Table II). Namely, PWB and Li-PWB have quite similar unit cell volumes, whereas Ca-PWB has significantly compressed unit cell and lower volume. Therefore, large cages formed by quite regular WO_6 octahedra and PO_4 tetrahedra sharing corners should be the smallest ones for the Ca-PWB in comparison to PWB and Li-PWB. The compressed Ca-PWB unit cell volume could indicate the difficult availability or demanding orientation of the active site for potential heterogeneous catalysis. Furthermore, it was previously shown that various tilting and orientations of the polyhedrons and polyhedral chains in other phosphate tungsten bronzes could derive the different space groups of crystallization [5], which makes this problem very complex from the structural aspect. The similar observations were also confirmed in our studies of other materials [38, 39]. Although crystal structure refinements were beyond of the scope of this paper, different calculated crystallographic axis and angles between PWB, Li-PWB, and Ca-PWB (Table II) could be sufficient proof of the various tilting of their WO_6 octahedrons and PO_4 tetrahedrons. Such tilting is obviously caused by different inserted cations into the structure, leading to their different active sites accessibility and consequently different catalytic activity in the BR system.

The aim of catalysis is enhancement of the particular reaction rate towards increasing reaction rate constant (k) and decreasing of the apparent activation energy (E_a) decreases [40]:

$$k = A \times e^{\frac{-E_a}{RT}} \quad (2)$$

where, k is rate constant, A is pre-exponential factor, R is universal gas constant, 8.314 kJ mol^{-1} and T is absolute temperature. The slope of the relative τ_{osc} vs. added bronze mass curve should be directly related to the efficiency of catalyst (Fig. 7). If slope is larger, the performance of the catalyst is better (the reaction is more accelerated), for the oxidation process involving hydrogen peroxide in the BR reaction. Consequently, the catalytic activity of investigated bronzes should be as followed: PWB > Li-PWB >> Ca-PWB. The apparent

activation energy of a particular oxidation reaction involving hydrogen peroxide in the BR system in the presence of phosphate tungsten bronzes decreased in following order E_a (Ca-PWB) >> E_a (Li-PWB) > E_a (PWB). Hence, the "BR slope" might be considered as a potential new parameter for the evaluation of catalytic activity in the oxidation process involving hydrogen peroxide with potential application in green catalytic engineering [41-43]. Furthermore, it is easy way to investigate direction of catalyst development. In here investigate case, the phosphate tungsten bronzes doping with monovalent and divalent cation impairs catalytic ability. Therefore, according to the Briggs-Rauscher reaction, the doping with Li and Ca should not been considered as potential method in the improvement of the catalytic activity of phosphate tungsten bronzes towards oxidation processes including hydrogen-peroxide. The oscillatory BR reaction has been shown as a novel rapid screening test of bronzes (catalytic) properties.

4. Conclusion

The thermally phase transformation of calcium salts of 12-tungstophosphoric acid in order to obtained novel Ca-doped phosphate tungsten bronze has been presented and characterized. The influence of new synthesized Ca-PWB, as well as Li-PWB and cation free PWB bronzes on the BR reaction dynamics has also been compared. The results evidently show that doping with Li and Ca reduces sensitivity (decrease the slope of τ_{osc} vs. mass curve) of BR reaction towards bronzes addition. Furthermore, the doping with a divalent cation Ca^{2+} significantly changes the properties of cation-free PWB. The obtained results strongly suggest the usage of the BR oscillatory reaction as an innovative method for testing different catalytic properties of bronzes. The reasons for different bronzes' catalytic activity were found in their calculated unit cell volumes. Namely, PWB and Li-PWB has quite similar unit cell volumes, whereas Ca-PWB has significantly compressed unit cell and lower volume. The compressed Ca-PWB unit cell volume could indicate the difficult availability (or demanding orientation) of the active site for heterogeneous catalysis. Additionally, the linear correlation (particularly slope) of oscillatory time duration vs. mass of added catalyst (besides bronzes) in BR reaction might be considered as a new parameter for the evaluation of the catalytic activity of different catalysts in oxidation process involving hydrogen peroxide.

Acknowledgments

This work was financially supported by the Ministry of Education, Science and Technological Development of the Republic of Serbia (Grant No. 451-03-68/2020-14/200026, Grant No. 451-03-68/2020-14/200146 and Grant No. 451-03-68/2020-14/200122). This work is dedicated to Prof. dr Ubavka B. Mioč, Faculty of Physical Chemistry, University of Belgrade, who recently passed away and had devoted most of her professional work and life to studying phosphate tungsten bronzes.

5. References

1. O. Nakamura, T. Kodama, I. Ogino, Y. Miyake, Chem. Lett. 8 (1979), 17.
2. R. C. T. Slade, H. A. Pressman, E. Skou, Solid State Ion. 38 (1990), 207.
3. K. D. Kreuer, M. Hampele, K. Dolde, A. Rabenau, Solid State Ion. 28-30 (1988), 589.
4. U. B. Mioč, R. Ž. Dimitrijević, M. M. Mitrović, Z. P. Nedić, J. Serb. Chem. Soc. 60 (1995) 959.

5. P. Roussel, O. Pérez, P. Labbé, Acta Crystallogr. B. 57 (2001) 603.
6. Z. S. Teweldemethin, K. V. Ramanujachary, M. Greenblat, J. Solid State Chem. 95 (1991) 21.
7. F. E. L. Rodríguez, A. Martínez-de la Cruz, E. López Cuéllar, J. Power Sources. 160 (2006) 1314.
8. A. Martínez-de la Cruz, F. E. L. Rodríguez, Electrochim. Acta. 54 (2009), 3176.
9. E. Wang, M. Greenblat, J. Solid State Chem. 68 (1987), 38.
10. U. B. Mioč, R. Ž. Dimitrijević, M. Davidović, Z. P. Nedić, M. M. Mitrović, Ph. Columban, J. Mater. Sci. 29 (1994) 3705.
11. R. Ž. Dimitrijević, Ph. Columban, U. B. Mioč, Z. Nedić, M. R. Todorović, N. Tjapkin, M. Davidović, Solid State Ion. 77 (1995) 250.
12. M. Vujković, Z. Nedić, P. Tančić, O. S. Aleksić, M. V. Nikolić, U. Mioč, S. Mentus, J. Mater. Sci. 51 (2016) 2481.
13. B. Broyde, J. Catal. 10 (1968) 13.
14. X. Du, Y. Pu, X. Peng, R. Li, Ceram. Int. 46 (2020) 11492.
15. G. Wang, Q. Fu, H. Shi, F. Tian, P. Guo, L. Yan, S. Yu, Z. Zheng, W. Luo, J. Am. Ceram. Soc. 103 (2020) 2520.
16. L. Moore, I. Dutta, B. Wheaton, E. Stapleton, R. Parysek, B. Aitken, J. Am. Ceram. Soc. 103 (2020) 3552.
17. M. C. Pagnacco, J. P. Maksimović, T. M. Mudrinić, Z. D. Mojović, Z. P. Nedić, J. Electroanal. Chem. 849 (2019), 113369.
18. T. V. Maksimović, J. P. Maksimović, Lj. G. Joksović, Z. P. Nedić, M. C. Pagnacco, Chem. Ind. 72 (2018), 275.
19. T. S. Briggs, W.C. Rauscher, J. Chem. Educ. 50 (1973) 496.
20. R. J. Field, J. Chem. Educ. 77 (2000) 450.
21. J. P. Maksimović, Ž. D. Čupić, D. Lončarević, N. Pejić, D. Vasiljević-Radović, S. Anić, Sci. Sinter. 43 (2011) 55.
22. G. Schimitz, Z. Noszticzius, G. Hollo, M. Wittmann, S.D. Furrow, Chem. Phys. Lett. 691 (2018) 44.
23. G. Schmitz, Phys. Chem. Chem. Phys. 3 (2001) 4741.
24. D. R. Stanisavljev, M. C. Milenković, M. D. Mojović, A. D. Popović-Bijelić, J. Phys. Chem. A. 115 (2011) 2247.
25. M. C. Milenković, D.R. Stanisavljev, Russ. J. Phys. Chem. 85 (2011) 2279.
26. M. C. Milenković, D.R. Stanisavljev, J. Phys. Chem. A. 116 (2012) 5541.
27. R. Cervellati, K. Höner, S. D. Furrow, C. Neddens, S. Costa, Helv. Chim. Acta. 84 (2001) 3533.
28. Ž. D. Čupić, Lj. Z. Kolar-Anić, S. R. Anić, S. R. Maćešič, J. P. Maksimović, M. S. Pavlović, M. C. Milenković et al., Helv. Chim. Acta. 97 (2014) 321.
29. I. N. Bubanja, M. C. Pagnacco, J. P. Maksimović, K. Stevanović, D. R. Stanisavljev, React. Kinet. Mech. Cat. 123 (2018) 47.
30. J. P. Maksimović, J. Tošović, M.C. Pagnacco, Bull. Chem. Soc. Jpn. 93 (2020) 676.
31. U. Mioč, Ph. Columban, A. Novak, J. Mol. Struct. 218 (1990) 123.
32. R. Garvey, Least-square unit cell refinement, Version 86.2., Department of Chemistry, North Dakota State University, 1987.
33. S. Stašoć, D. Božić, Sci. Sinter. 52 (2020) 15.
34. S. Milanović, N. Potkonjak, V. Mandušić, Đ. Čokeša, J. Hranisavljević, B. Kaluđerović, Sci. Sinter. 52 (2020) 87.
35. R. Davodi, M. Ardestani, A. Kazemi, Sci. Sinter. 52 (2020) 245.
36. N. Obradović, W. G. Fahrenholtz, S. Filipović, C. Corlett, P. Đorđević, J. Rogan, P. J. Vulić, V. Buljak, V. Pavlović, Sci. Sinter. 51 (2019) 363.

37. C. Venturello, R. D'Aloisio, J. C. J. Bart, M. Ricci, J. Mol. Catal. 32 (1985) 107.
38. P. Tančić, R. Dimitrijević, M. Poznanović, A. Pačevski, S. Sudar, Acta Geol. Sin-Engl. 86 (2012) 1524.
39. P. Tančić, A. Kremenović, P. Vulić, Powder Diffr. 35 (2020) 7.
40. S. Anić, M. Kostić, M. Ninić, S. Blagojević, Lj. Kolar-Anić, Sci. Sinter. 39 (2007) 77.
41. R. Noyori, M. Aoki, K. Sato, Chem. Commun.16 (2003) 1977.
42. S. P. Teong, X. Li, Y. Zhang, Green Chem. 21 (2019) 5753.
43. N. M. Deraz, Sci. Sinter. 52 (2020) 53.

Сажетак: *У овом раду синтетисана је и окарактерисана (TGA, DSC, XRPD, FTIR, SEM) нова калцијумом допирана фосфат волфрамова бронза (Ca-PWB). Испитан је и упоређен утицај фосфат волфрамове бронзе (PWB), литијумом допиране фосфат волфрамове бронзе (Li-PWB) и калцијумом допиране фосфат волфрамове бронзе (Ca-PWB) на осцилаторну динамику Briggs-Rauscher (БР) реакције. Резултати показују да допирање катјонима* Li^{+} *и* Ca^{2+} *смањује осетљивост БР реакције на додатак нерастворних бронзи, што се огледа у смањивању нагиба праве осцилаторног времена* (τ_{osc}) *БР реакције у функцији масе додате допиране бронзе. Добијени резултати сугеришу употребу БР реакције као иновативне методе за испитивање различитих својстава допираних и недопиране фосфат волфрамове бронзе. Разлози за различито понашање бронзи у осцилаторној реакцији пронађени су у различитим величинама јединичних ћелија PWB, Li-PWB и Ca-PWB. Наиме, најмања вредност, тј. сабијање јединичне ћелије допирањем калицијумом указује на тежу доступност активних места за хетерогену катализу. Каталитичка активност бронзи усмерена је ка реакцијама оксидације које укључују водоник-пероксид (један од реактаната БР реакције). Стога би се линеарна корелација (нагиб) tosc у функцији масе бронзе у БР реакцији могла сматрати новим параметром за процену каталитичке активности бронзе, али и других материјала.*

Кључне речи*: Бригс-Раушерова реакција; Фосфат-волфрамове бронзе; Кегинове структуре, Каталитичка активност; Хетерогена катализа.*